Article:

Fogt, R.L., Jones, J.M. orcid.org/0000-0003-2892-8647, Goergens, C.A. et al. (3 more authors) (2016) Antarctic station-based seasonal pressure reconstructions since 1905: 2. Variability and trends during the twentieth century. Journal of Geophysical Research: Atmospheres, 121 (6). pp. 2836-2856. ISSN 2169-897X

https://doi.org/10.1002/2015JD024565

Antarctic station based seasonal pressure reconstructions since 1905: 2. Variability and trends during the twentieth Century

Ryan L. Fogt[1], Julie M. Jones[2], Chad A. Goergens[1], Megan E. Jones[1], Grant A. Witte[1], and Ming Yueng Lee[1]

[1]Department of Geography and Scalia Laboratory for Atmospheric Analysis, Ohio University, Athens, OH, USA
[2]Department of Geography, University of Sheffield, Sheffield, United Kingdom

Corresponding author address: Ryan L. Fogt, 122 Clippinger Laboratories, Department of Geography, Ohio University, Athens, OH, 45701. Email: fogtr@ohio.edu

KEY POINTS:

1. Austral summer is marked with strong interannual pressure variability in the early 20th century across Antarctica.
2. Recent trends over the last ~30 years in austral summer are unique across the entire content in the context of the entire 20th century.
3. Winter pressure variability is much less variable and more regional in nature in the early 20th century, compared to austral summer.

Abstract

The Antarctic seasonal station-based pressure reconstructions evaluated in our companion paper are here evaluated to provide additional knowledge on Antarctic pressure variability during the 20th century. In the period from 1905-1956, we find that the Hadley Centre gridded sea level pressure dataset compared the best with our reconstructions, perhaps due to similar methods to estimate pressure without direct observations.

The primary focus on 20th century Antarctic pressure variability was in summer and winter, as these were the seasons with highest reconstruction skill. In summer, considerable interannual variability, and these variations were spatially uniform across all of Antarctica. Notable high pressure anomalies were found in the summers of 1911/12 and 1925/26; both summers correspond to negative phases of the Southern Annular Mode as well as El Niño events in the tropical Pacific. In addition, negative summer pressure trends during the last ~40 years across all of Antarctic are unique in the context of 30-year trends throughout the entire 20th century, suggesting a strong component of anthropogenic forcing on the recent summer trends. In contrast, mean winter pressure is less variable from year to year during the early 20th century, and there are less similarities between these pressure variations along the Antarctic Peninsula compared to the rest of the continent. No significant pressure trends were found consistently across all Antarctica (although some significant regional trends can be identified), and low-frequency, multi-decadal scale variability appears to dominate the historical pressure variations in this season.

1. Introduction

Due to the lack of long-term observations, the scientific understanding of early 20th century Antarctic atmospheric circulation variability is more limited than anywhere else on Earth. While early expeditions and Antarctic explorers, as well as whaling ships, provide clues into some meteorological conditions, these details are discontinuous in time and space and are often qualitative (describing conditions of sea ice, wind, or temperature) rather than direct measurements of the atmosphere. South of 60°S, only one station has a continuous record extending back to 1903- the station Orcadas, located northeast of the Antarctic Peninsula (60.7°S, 44.7°W). *Zazulie et al.* [2010] analyzed the daily temperature record at Orcadas, and noted that there were no statistically significant temperature trends prior to 1950 for any season; in contrast, statistically significant warming was found in all seasons in the latter half of the 20th century. Similarly, *Murphy et al.* [2014] examine winter fast-ice conditions nearby in the north Weddell Sea during the twentieth century and find strong interannual variability in the formation and breakout dates related to atmospheric circulation changes manifested in the Southern Annular Mode (SAM) or the El Niño – Southern Oscillation (ENSO) teleconnection. While these studies increase the understanding of 20th century Antarctic climate variability, they are only at a single location and are likely not representative of conditions across all of Antarctica. While the European Centre for Medium Range Weather Forecasts (ECMWF) 20th century reanalysis (ERA-20C), the Hadley Centre gridded mean sea level pressure version 2 [HadSLP2; *Allan and Ansell*, 2006], and the National Oceanic and Atmospheric Administration 20th – Cooperative Institute for Research in Environmental Studies (NOAA-CIRES) century reanalysis, version 2c [20CR, *Compo et al.*, 2011], provide gridded pressure values into the early 20th century, these have essentially very little data constraints south of 60°S prior to 1957, and therefore are often unreliable in this region. Evaluations of these products demonstrate that either the number of observations incorporated decreases dramatically in HadSLP2 [*Allan and Ansell*, 2006] or the ensemble variance [a measure of the reliability of the 20CR, *Compo et al.*, 2011] becomes very large in the high southern latitudes in the period 1900-1950. Both studies urge caution in interpreting these products near and over Antarctica during this time period, and as such the gridded climatologies do not provide much guidance in interpreting early 20th century Antarctic climate variations.

Additional sources of century-length Antarctic climate variability come from reconstructions of the Southern Annular Mode index from observations [*Jones et al.*, 2009; *Visbeck*, 2009], tree rings [*Jones and Widmann*, 2003, 2004; *Villalba et al.* 2012] and ice cores [*Abram et al.*, 2014], which provide estimates on large-scale Southern Hemisphere atmospheric circulation variability back to at least the early 20th century. Although there are differences among these reconstructions, all indicate the uniqueness of positive SAM index trends during the latter half of the 20th century, compared to a relatively neutral SAM index / weak trends during the early part of the 20th century. Based on how the SAM index is defined, these positive trends suggest pressure decreases across Antarctica; however the reconstructions are unable to provide information including both the spatial and temporal variability of the pressure trends (prior to direct observations) at specific locations across Antarctica. Climate models are used frequently to understand Antarctic variability across the 20th century [for example, *Arblaster and Meehl*, 2006; *Ding et al.*, 2011; *Fogt and Zbacnik*, 2014; *Fogt and Wovrosh*, 2015;

Perlwitz et al., 2008; *Turner et al.*, 2009; *Wilson et al.*, 2014; *Turner et al.*, 2015a], but again atmospheric, ocean, or sea ice conditions (depending on the scenario / simulation) cannot be precisely prescribed over the full century, and fully coupled models have been found to have notable differences from observations even in the latter part of the 20^{th} and early 21^{st} centuries [*Hosking et al.*, 2013; *Turner et al.*, 2013; *Bracegirdle et al.*, 2014; *Bracegirdle et al.*, 2016; *Marshall and Bracegirdle*, 2015; *Turner et al.*, 2015b]. Climate information extracted from ice cores can also provide information on Antarctic climate variability. Focusing on the 20^{th} century, some of these studies have demonstrated significant warmth along the Antarctic Peninsula in the 1940s [*Schneider and Steig*, 2008]; a decline of sea ice extent in the Bellingshausen Sea [*Abram et al.*, 2010]; a doubling of snow accumulation across the western Antarctic Peninsula [*Thomas et al.*, 2008]; and time-varying relationships between the SAM and temperature along the Antarctic Peninsula [*Marshall et al.*, 2011].

Given the knowledge gaps that still exist and the large role of natural variability in the Antarctic climate system, the station-based seasonal pressure reconstructions presented in the companion paper [*Fogt et al.*, 2016] provide a unique opportunity to understand atmospheric circulation variability across all of the Antarctic continent during the entire 20^{th} century. This is especially true since the summer (original) and winter (pseudo-proxy) reconstructions were found to be of high quality through the extensive evaluations performed in our companion paper [*Fogt et al.*, 2016]. We first compare the reconstructions to other gridded pressure data, before examining historical pressure variability across Antarctica (including relationships with both ENSO and SAM), and conclude by examining Antarctic pressure trends during the 20^{th} century.

2. Data and Methods

We make extensive use of the seasonal pressure reconstructions discussed and evaluated in *Fogt et al.* [2016]. These reconstructions were conducted at 18 stations across Antarctica; however, we only partly investigate the 20th century pressure variability using the Byrd reconstruction as this station tended to have a lower reconstruction skill due in part to its distance from midlatitude predictor stations, but also due to a data gap during most of the 1970s. In all cases, we employ the best 'full period' reconstructions from the various methods tested in *Fogt et al.* [2016]; similarly we also use the best performing 'pseudo-reconstructions' (between the pseudoproxy data from 20CR or HadSLP2). The focus is primarily on the winter and summer seasons, as these are the seasons with the highest reconstruction skill.

The location of the Antarctic stations investigated further is given here in Fig. 1. Because the pressure at many stations is strongly correlated in both the observations and reconstructions [cf. Fig. 7 of *Fogt et al.* 2016], in many cases regionally averaged seasonal pressures are investigated rather than individual stations. The coloring in Fig. 1 indicates these geographic regions of Antarctica: the western Antarctic Peninsula (Faraday, Rothera); the northern Antarctic Peninsula (Bellingshausen, Esperanza, O'Higgins / Marsh, Marambio); Dronning Maud Land (Halley, Novolazarevskaya, Syowa); coastal East Antarctica (Mawson, Davis, Mirny, Casey); the Ross Sea region (Dumont d'Urville, McMurdo / Scott Base); and the Antarctic Interior / Plateau (Amundsen-Scott, Vostok). Averaging over these pairs of stations acts only to simplify the main patterns of Antarctic pressure variability over the 20th century and does not significantly alter the conclusions. In most cases, it also strengthens the agreement between the mean reconstructions and mean observations within the region compared to the individual reconstruction / observations pairs, therefore improving the accuracy of the reconstructions and as a result our understanding of historical Antarctic pressure variability and trends in the 20th century.

As discussed earlier, we use the reconstructions as a way to demonstrate the differences in other measures of historical Antarctic pressure variability by comparing them to the gridded products of HadSLP2, 20CR, and ERA-20C. We employed 5°x5°, 2°x2°, and 1.5°x1.5° latitude-longitude monthly sea level and surface pressure data from HadSLP2, 20CR, and ERA-20C, respectively (no surface pressure data are available for HadSLP2), and constructed seasonal means from these data. All the gridded data extend through at least 2010, and over the interior of the Antarctic continent surface pressure was used for direct comparison to the reconstructions instead of sea level pressure since the reduction to sea level is unreliable on the high ice sheet. All seasons are defined based on the Southern Hemisphere: December-February (DJF) for summer, March – May for autumn (MAM), June – August (JJA) for winter, and September – November (SON) for spring.

3. Results

3.1. Comparisons to gridded pressure data

Before investigating the 20th century seasonal pressure variability, we first conducted comparisons of the gridded pressure data to the reconstructions. The gridded data were bilinearly interpolated to the latitude / longitude of the stations in Fig. 1, and the correlation, bias, and root mean squared error (RMSE) between HadSLP2, 20CR, and

ERA-20C were calculated by season. Since we expect the quality of these gridded data to improve with the assimilation of the Antarctic pressure and other observations, most of which began near the International Geophysical Year (1957-1958), we calculate these statistics over two separate time periods: the 'early' period being 1905-1956, and the 'late' period consisting of 1957-to the end of the gridded data or reconstruction, which varies between 2010-2013. These statistics are displayed in Fig. 2, with the x-axis identifying the station, working east around Antarctica starting at the Antarctic Peninsula station Rothera (Fig. 1). In Fig. 2, we only investigate comparisons with the original reconstructions in order to avoid any circularity (i.e., using some of the products to evaluate themselves). However, because the reconstructions are less reliable in MAM and SON, it is somewhat misleading to provide an evaluation of the various products' skill in the transition seasons (since the reconstructions differ more from observations). Rather, in MAM and JJA Fig. 2 is more of an evaluation of how similar the variability is in the reconstructions and the gridded products throughout the 20th century.

In summer, when reconstruction skill is high across all of Antarctica, correlations during the later part of the 20th century are generally above 0.8 for all stations. However, there is a marked decrease in the early 20th century, and only HadSLP2 produces correlations above 0.4 near the Antarctic Peninsula (stations 1-6). All products have notably different early 20th century variability than the reconstructions across nearly all the coastal stations (from Halley east through Dumont d'Urville, stations 7-14); correlations with ERA-20C and the reconstructions are negative at all of these stations, suggesting a notably different pattern of variability in this reanalysis from the late to early 20th century (compared to the reconstructions, which reproduce the observations well).

While all products have near-zero bias in summer (middle column of top row), ERA-20C again has a much higher positive bias than other products, on the order of 6-8 hPa higher. With the lower correlation and higher bias, the RMSE during the early 20th century in ERA-20C also stands out as an outlier. Notably, HadSLP2, the coarsest data set, has much more consistent RMSE values in the early and later parts of the 20th century when compared to the reconstructions, which suggests this product provides a similar range of variability as the reconstructions, and is consistent with them throughout the entire 20th century.

Although the reconstruction performance is weaker in the non-summer seasons, the skill remains high across the Antarctic Peninsula in all seasons [*Fogt et al.*, 2016]. For these locations (stations 1-6 on the x-axis), there are again smaller changes in correlation, bias, and RMSE in HadSLP2 between the early and late portions of the 20th century compared to 20CR and ERA-20C; this is true in every season for the Antarctic Peninsula stations. Broadly, for the other locations, there is a general pattern across all seasons that ERA-20C agrees the least with the reconstructions across all of the stations on the Antarctic coast, that 20CR has a much lower surface pressure at Vostok (station 16), and that HadSLP2 has the least changes in all statistics between the early and late portions of the 20th century. Further, it is also apparent that while the agreement between the reconstructions and these products is roughly consistent across all stations during the later part of the 20th century (when the observations better guide the gridded products), there is a marked decrease in the similarities between the reconstructions and these products in the earlier 20th century at all coastal Antarctic stations (i.e., ‘early’ correlations consistently drop across stations 6-14, and biases and RMSEs increase). As noted before, these changes suggest a marked difference in the variability of these gridded products compared to the reconstructions during the early 20^{th} century. Indeed, there is a notable change in the mean and variance in these gridded products with time that is not reflected in the reconstructions [*Allan and Ansell*, 2006; *Compo et al.*, 2011]. Altogether, Fig. 2 highlights that the HadSLP2 product most directly compares to the reconstructions at all locations, while the largest differences are from the most recent, and highest resolution ERA-20C pressures. Although this may seem surprising, HadSLP2 is based on a principal component reconstruction technique to infill data over large spatial gaps [*Allan and Ansell*, 2006], and since this method is similar to the method employed in producing the reconstructions, the similarities may simply reflect a likeness in approach rather than implying that HadSLP2 provides the best estimate of 20^{th} century Antarctic pressure variability. The remainder of this study will focus solely on summer and winter pressure variability during the 20^{th} century, due to the higher reconstruction skill in these seasons.

3.2. 20^{th} century sea level pressure variability

The time series of the interannual summer sea level pressures, regionally-averaged following Fig. 1, are presented in Fig. 3 from observations (black lines) and the best original (red lines) and pseudoproxy-based reconstructions (blue lines). As an estimate of the uncertainty in the reconstructions, the gray shading represents the maximum and minimum extent of the 95% confidence intervals from both the original and pseudo-reconstructions. These confidence intervals were calculated as 1.96 times the standard deviation of the residuals between the regionally-averaged observations and reconstructions from 1957-2013. Also provided in Fig. 3 are the correlations between the regionally-averaged observations and original/pseudo reconstructions over the same time period; in DJF these are generally above 0.90 except for the Ross Sea region (Fig. 1).

There are many interesting observations when examining the Antarctic 20th century pressure variability in summer. First, there is a strong consistency across all stations in terms of the variability throughout the entire century in both observations and reconstructions. This reflects the overall weaker structure of the circumpolar jet, the continual input of solar radiation at these locations in summer, and the tendency for the SAM to have a zonally symmetric structure in summer [*Fogt et al.*, 2012]. Second, there are many interesting sharp interannual changes in sea level pressure, particularly during the summers of 1911/12, 1925/26, and the transition from low pressure values in 1960/61 to moderately high values in 1961/62 the following year. Third, based on the minima of the historical 95% confidence intervals on the reconstructions, many of the observed low pressure values during the late 1990s and in the 2000s are either the absolute lowest, or among the lowest summer pressures seen since 1905 (especially away from the Antarctic Peninsula, Figs. 3c-e). Lastly, there are notable decreases in the pressure at all stations since ~1960, which will be discussed in more detail in section 3.5.

With doubling the length of the observations through the reconstructions, it is clear that summer pressure historically is more variable than the observations indicate since 1957. While the change from the low-pressure values in summer 1960/61 to the high values in 1962/63 has been discussed in context of SAM index changes from high to low values, respectively, and thought to be due to the Agung eruption [*Marshall*, 2003], the sudden sea level pressure spikes across all of Antarctica in the summers of 1911/12 and 1925/26 are unique pressure changes that have no strong similarity during the period of observations. We investigate the 1925/26 event here in more detail, as a separate study is ongoing for the 1911/12 summer since this was the time of the Amundsen and Scott expeditions to the South Pole [*Solomon and Stearns*, 1999].

Figure 4 displays the 1925/26 sea level pressure anomalies (contoured, standardized anomalies from the 1981-2010 mean are shaded) from the gridded products of 20CR, ERA-20C, and HadSLP2, as well as the anomalies from observations in the midlatitudes and the original reconstructions in Antarctica. While there are fairly large differences between the gridded products in terms of the magnitude and location of regional features, the overall spatial pattern is remarkably similar, reflecting high pressures over the entire Antarctic continent and lower pressures over much of the midlatitude Southern Hemisphere between 30°-60°S. This pattern reflects a strongly negative SAM index state, and indeed historical reconstructions of the SAM index [*Jones et al.*, 2009] based on both the 'Fogt' and 'JW concat' reconstructions are all strongly negative in DJF 1925/26 (-3.25 and -1.96, respectively). Furthermore, the Southern Oscillation Index (a measure of ENSO activity) from the NOAA Climate Prediction Center (ftp://ftp.cpc.ncep.noaa.gov/wd52dg/data/indices/soi.his) was moderately negative (-2.07) during summer 1925/26, indicating El Niño conditions in the tropical Pacific. This is reflected also in the SLP contours in Fig. 4, with negative pressures in the central Pacific (including the station Tahiti), and positive pressure anomalies over Australia, reflecting the Southern Oscillation [*Trenberth and Caron*, 2004]. Regarding the spatial structure of the 1925/26 pressure anomaly field over Antarctica, the pressures are highest over the Antarctic Peninsula and West Antarctica, reflecting a weakening of the

Amundsen Sea Low, common during El Niño events [*Turner*, 2004; *Karoly*, 1989]. Spatially, HadSLP2 has the most consistent representation of the pressure anomalies seen in the reconstructions, including the slightly weaker anomalies in portions of coastal East Antarctica (less than 6 hPa above the mean), and the local region of a high pressure anomaly in the Weddell Sea (Fig. 4c). While the 20CR also has a region of higher pressure anomalies >8 hPa in the Weddell Sea, these extend too far eastward, as indicated by the pressure anomalies of 4-6 hPa at Novolazarevskaya and Syowa in the reconstructions. Notably, ERA-20C produces substantially higher sea level pressure anomalies south of 60°S (>16 hPa) compared to 20CR or HadSLP2 (which typically range from 4-8 hPa over Antarctica). These representations are consistent with the performance of the gridded products compared to the reconstructions discussed previously for Fig. 2. Nonetheless, the reconstructions and even the gridded pressure datasets, all indicate that summer 1925/26 was a unique year with much higher than normal pressures across all of Antarctica.

Low-frequency pressure variations in summer over the 20th century are plotted in Fig. 5. Here, the interannual pressure values from Fig. 3 have been smoothed with an 11-yr Hamming filter. In Fig. 5 the confidence intervals are based on the residuals from the smoothed reconstructions compared to the smoothed observations during 1957-2013 (rather than also smoothing the confidence intervals in Fig. 3, which would generate a much larger confidence interval that doesn't reflect the high ability of the reconstructions to capture the low-frequency observed variability, as indicated by the correlations in Fig. 5). While there appears to be larger differences between the two reconstructions, the y-axis is on a different scale and throughout nearly all of the 20th century the absolute difference is typically < 1 hPa. Further, the correlations between the reconstructed and observed pressures are all above 0.90 (most are above 0.95). Key features of the low-frequency summer pressure variability are 1) a prolonged period of lower pressure during the period 1915-1920 across all of Antarctica, 2) very little decadal-scale variability across most of Antarctica during 1920-1955 (the smooth reconstructions change generally less than 2 hPa during this time), and 3) negative pressure trends with embedded more marked regional variability (especially along the Antarctic Peninsula) since ~1965. In contrast to the low pressure values seen during the late 1990s and throughout the 2000s in many locations in Fig. 3, Fig. 5 highlights that the recent smoothed, low-frequency variations are not unique and are comparable to the variations during the early portion of the 20th century.

The interannual, regionally-averaged winter sea level pressures are shown in Fig. 6. There are many notable differences in the representation of winter 20th century Antarctic pressure variability compared to summer based on the reconstructions. First, the interannual winter pressure variability from the Antarctic Peninsula is much less correlated to the rest of the Antarctic continent than it was in the summer (Figs. 3, 6). Second, in stark contrast, the interannual variability is much higher over the latter half of the 20th century, when observations are available, than in the early part of the 20th century; while the pressure continues to change several hPa from year to year (Fig. 6), there are no sudden spikes that were seen at least two times in the early 20th century in DJF (Fig. 3). Third, there appears to be no persistent pressure trends as noted in summer.

The lack of consistency in the reconstructions across all areas in winter makes it challenging to focus on a single event for further study. However, in 1938 the pressures were among the lowest in the early 20th century across the Antarctic Peninsula (Figs. 6a-b), and the original reconstructions at least show below-average pressure across the rest of Antarctica. This year is examined further in Fig. 7 (as in Fig. 4), but with the pseudo-reconstructions plotted over Antarctica since they have the highest correlations with observations (*Fogt et al.*, 2016; Fig. 6). Immediately apparent in Fig. 7 are the much larger differences between 20CR, ERA-20C and HadSLP2, especially south of 60°S. Only HadSLP2 captures the negative pressure anomalies (<-2 hPa) across the Antarctic Peninsula; 20CR only has them along the northern Peninsula where they are the weakest, while ERA-20C has positive anomalies everywhere across the Peninsula, including the station Orcadas, which is an actual observation and not a reconstruction in Fig. 7. Based on the Fogt reconstruction, JJA 1938 was a positive SAM index year (2.688), which is consistent with most of the Antarctic stations showing negative pressure anomalies. Further, the SOI was moderately positive (1.37), indicating La Niña conditions, also consistent with the negative pressure anomalies along the Antarctic Peninsula [especially the western Peninsula, *Clem and Fogt*, 2013], and Byrd station in West Antarctica, associated with a deepening of the Amundsen Sea Low in La Niña events [*Turner*, 2004]. Combined with the pseudo-reconstruction calibrations correlations >0.87 (Fig. 6), more confidence is therefore placed on the spatial pressure anomaly pattern over Antarctica by the reconstructions than the gridded products, which all show positive pressure anomalies in coastal East Antarctica and Dronning Maud Land. Over the interior, pressure anomalies are near-zero in the reconstructions (except at Byrd in West Antarctica), and therefore ERA-20C may actually provide the best depiction in the Antarctic interior for this event (it is the only dataset to show negative anomalies in the South Pacific associated with the La Niña event), with HadSLP2 providing the best representation along the Antarctic Peninsula. Nonetheless, given these discrepancies, it is clear that the reconstructions provide crucial information in understanding the early 20th century pressure variations across Antarctica beyond that from current gridded datasets.

The low-frequency (smoothed) winter sea level pressures are shown in Fig. 8. There are larger differences between the two reconstructions in the early 20th century in part because of the lower skill in the original reconstructions, and differences approach 3 hPa at times (particularly in the Ross Sea region, Fig. 8e); nonetheless, some general patterns of the low-frequency variability can be discussed. In particular for every region except Dronning Maud Land, the smoothed reconstructions and observations in the later part of the 20th century all have much more of a oscillatory behavior, highlighting that decadal-scale variability is more prevalent in winter pressures across Antarctica than in summer. These oscillations are perhaps most marked near the Antarctic Peninsula and Ross Sea region, and may reflect historical decadal-scale ENSO variability as seen in previous studies [*Fogt and Bromwich*, 2006; *Stammerjohn et al.*, 2008; *Fogt et al.*, 2011]. Changes in this type of variability will be examined in section 3.4.

3.3. Surface pressure variability on the Antarctic Plateau

Since the reduction to sea level pressure is unreliable on the high Antarctic Plateau / Interior, surface pressure was reconstructed for the interior stations. However, the mean surface pressure varies considerably between Amundsen-Scott and Vostok, as the latter is about 650m higher in elevation. To compare the historical pressure variability at these stations, the mean surface pressure during 1981-2010 was removed, and the resulting anomaly time series for the two stations were averaged. Fig. 9 displays the mean Antarctic Plateau surface pressure anomalies for summer and winter, along with the 11-yr smoothed low-frequency versions. In general, the pseudo-reconstructions perform as well as the original in summer, but the pseudo-reconstructions have considerably higher skill in winter [*Fogt et al.*, 2016]. Figure 9 demonstrates that while the interannual variability is consistently marked over the 20th century in summer (Fig. 9a), the interannual variability is reduced considerably during the early parts of the 20th century in austral winter (Fig. 9c), as observed for other Antarctic regions in Fig. 6. In summer, several above-average pressure anomalies occur during the early 20th century, in agreement with those at coastal stations, reflecting a negative SAM structure (Figs. 9a, 3, and 4). From the low-frequency variability, most of the 20th century was marked with positive surface pressure anomalies across the Antarctic interior, highlighting the uniqueness of the recent negative values in the late 20th and early 21st centuries in summer (Figs. 9a-9b). This is in contrast to austral winter, which despite the differences in the reconstructions, both indicate low-frequency (i.e., multi-decadal) fluctuations above and below the mean (Fig. 9d), with a period of reduced interannual variability during 1930 – 1960 (Fig. 9c). Although the reconstructions at times differ on the sign of the anomalies in the winter (Figs. 9c-9d), the reduced variability is also seen in the winter observations (black line in Fig. 9c), although for shorter periods. While the reduced year-to-year variability in winter was discussed previously across coastal East Antarctica extending east to the Ross Sea Region (Figs. 4c-e), the changes from one winter to the next are even smaller across the Antarctic Plateau in the early to mid 20th century (Fig. 9c). This could be a reflection of the reduced reconstruction skill, or perhaps indicate that the atmosphere in the high interior becomes strongly stably stratified in winter, and may more frequently reach the climatologically average value during conditions when radiative equilibrium is more consistently achieved.

3.4. ENSO and SAM Pressure relationships during the 20th century

To examine the role of various Southern Hemisphere modes of climate variability on the 20th century pressure variability at the stations in Fig. 1, 30-year running correlations between ENSO and SAM indices were investigated. Running correlations are here defined as the correlation coefficient between a climate index calculated over a 30-year period, with the window moving forward a year, and the correlation recalculated; the concatenated series of all correlation values produce a time series. This is used to investigate changes in the roles of both ENSO and SAM throughout the 20th century, in particular because previous studies have noted varying temporal influences of each of the modes on aspects of the Antarctic climate [*Stammerjohn et al.*, 2008; *Clem and Fogt*, 2013; *Marshall et al.*, 2011; *Marshall and Bracegirdle,* 2015]. For the SAM index, running correlations between the pressures at each station with the 'Fogt' and 'JW concat' reconstructions [*Jones et al.*, 2009] were calculated individually and then averaged across the geographic regions in Fig. 1, and are displayed in Fig. 10 for austral summer (red lines) and winter (blue lines); dashed horizontal lines at $r = \pm 0.37$ represent the $p<0.05$ significance level, assuming independence of each seasonal mean. Notably, throughout the entire 20th century, there are only a few locations at very specific 30-year intervals where the SAM index correlations are not significant at $p<0.05$. These entirely occur in the non-summer seasons, when the reconstruction skill of both these SAM indices [*Jones et al.*, 2009] and the pressure at each station is slightly lower, especially during the early 20th century for the 'JW concat' reconstructions. For the Antarctic Peninsula (Figs. 10a-b), the winter correlations with the SAM index reconstructions become insignificant after 1940. This reduced relationship between the SAM and Antarctic Peninsula pressure reflects the seasonally-varying structure of the SAM [*Fogt et al.*, 2012], which has its largest asymmetry in winter near the Antarctic Peninsula. During this season, pressure anomalies in response to SAM events (especially SAM negative events) are shifted away from the Antarctic Peninsula [cf. Figs. 2-4 of *Fogt et al.*, 2012]. However, Figs. 10a-b suggest this relationship is not temporally persistent across the Antarctic Peninsula (where reconstruction skill is remains high in winter), with significant (p<0.05) negative SAM-pressure relationships across the Peninsula during the early 20th century. This may further explain some non-stationary SAM relationships seen in ice cores [i.e., *Marshall et al.*, 2011] or discrepancies between the Fogt reconstruction and SAM index reconstruction based on an ice core along the Antarctic Peninsula [*Abram et al.*, 2014]. In winter, Figs. 10a-b suggest a changing SAM structure to more zonally symmetric / uniform across the Antarctic Peninsula in the early 20th century to one with a weaker SAM influence during the latter part of the 20th century. Apart from this season and region, however, many of the SAM-pressure relationships are persistently significant (p<0.05) across the continent.

The story is quite different when examining the running correlations between the pressure reconstructions and the SOI. Several studies have noted changes in the ENSO-related climate influences that change through time [*Fogt and Bromwich*, 2006; *Stammerjohn et al.*, 2008; *Clem and Fogt*, 2013], and based on the running correlations between the SOI and the Antarctic pressure reconstructions (Fig. 11), these relationships continue to vary throughout the entire 20th century. In most cases, the correlations are not statistically significant, and no significant relationship persists for more than a 45-year period (or about 15 years on the x-axis of Fig. 11 accounting for the fact that these labels reflect the starting year of the 30-year correlations). Notably, recent significant negative correlations (i.e., lower pressure during La Niña years) across much of Antarctica during DJF weaken considerably before 1960, and in many cases reverse sign to weakly positive correlations. For winter, SOI correlations with pressure along the Antarctic Peninsula reflect those in summer, but the correlations between the two seasons are more opposite across the rest of the Antarctic continent. The contrast is most marked across coastal East Antarctica, where since 1970 the SOI is negatively correlated with pressure in summer, but positively correlated in winter. While the SOI correlations are generally much weaker in the earlier parts of the 20th century, the opposite correlations between winter and summer remain a consistent story (Fig. 2d). The differences likely reflect seasonal differences in the structure of the ENSO teleconnection between winter and spring, as noted by *Karoly* [1989]. However, since part of the ENSO teleconnection appears related to the phase of the SAM, they could also represent the seasonally varying SAM structure as well [*Fogt et al.*, 2011; *Fogt et al.*, 2012; *Wilson et al.* 2014].

3.5. Pressure trends during the 20th century

During the investigation of the interannual pressure reconstructions, it was apparent that most locations display negative pressure trends during the last 50 years. We finalize our discussion by examining these trends in more detail, using 30-year running trends for summer (Fig. 12) and winter (Fig. 13) for the reconstructions and observations. In each case, similar to the running correlations, trends were calculated at each station individually, and averaged over the regions denoted in Fig. 1, rather than taking the trends of the average pressure series (both methods produce similar results, however, due to the very similar interannual pressure variability at each station within a region). Here, the gray shading provides a measure of how well the reconstructions' trends align with the observations, as they are based on 1.96 times the standard deviation of the residuals between the 30-yr overlapping observed and reconstructed trends during 1957-2013. As with the interannual time series, the shading is based on the largest range between the original and pseudo reconstructions in order to more carefully represent the uncertainty in the earlier pressure trends.

The running trends for summer clearly demonstrate that the (observed and to a lesser extent reconstruction) negative pressure trends since ~1960 are unique over the last 100+ years across all of Antarctica, especially from Dronning Maud Land east toward the Ross Sea region (Fig. 1, Figs. 12c-e). Using the most negative trend estimates of the historical trends from both reconstructions (i.e., the bottom of the gray shading), the observed recent negative trends for all locations across Antarctica were the most negative they have ever been since 1905, especially for 30-year trends starting from 1965-1975. These negative trends are clearly seen in the interannual and low-frequency time series (Figs. 3-4), and their uniqueness over the last century strongly suggests that external forcing factors, rather than natural or internal climate variability, are playing a role in these negative trends. Previous work has highlighted in particular the role of ozone depletion on positive SAM index trends in austral summer, which would be consistent with the negative pressure trends seen since after the ozone hole formed [~1980; *Miller et al.*, 2006; *Perlwitz et al.*, 2008; *Fogt et al.*, 2009). Future work includes examining several climate model simulations to understand the relative roles of natural variability and forced changes from both greenhouse gases and ozone depletion on Antarctic pressure changes over the entire 20th century, and investigating these changes in greater detail.

In winter (Fig. 13), the recent trends appear not to be unique since 1905; not only have trends of similar magnitude been observed previously, but the change in trend from weakly negative to weakly positive that has occurred at most locations in the observations and reconstructions characterized much of the Antarctic winter pressure changes from 1915-1935. While there are differences in the magnitude of the pressure trends, both pseudo and original reconstructions generally show the trends becoming more positive over this time period, similar to the changes that have been occurring in the observations, except over the Antarctic interior. Here (Fig. 13f), the reconstruction skill is lower, and although the pseudo-proxy reconstructions improve the skill, there are still large differences early in the record (notably due to the fact that much of the 'pseudo' data extracted from HadSLP2 and 20CR was set to zero since there were much larger uncertainties in much of the early winter values for these over the open ocean). Despite this, the reconstructions suggest strong positive pressure trends during 1935-1965 from Dronning Maud Land east to the Ross Sea Region (Figs. 13c-e). Since the gray shading (a measure of the 95% confidence for the actual historical trend) rises above zero during this time, there is p<0.05 chance the reconstructed trends were actually negative (note this is not a statistical test on the actual measure of the trend, rather just the sign of the reconstructed trend based on reliability of both reconstructions in producing the observed trends). In all of these locations in Figs. 13c-e, the positive reconstructed trends during 1935-1965 are higher than any of the observed trends, and because they are not persistent (as the main forcing mechanisms such as greenhouse gas increases would be), the strong positive trends highlight the important role of natural variability in driving changing multi-decadal pressure trends across Antarctica in winter. Indeed, the general depiction of pressure trends during the 20th century from Fig. 13 is a continual change from increasing trends (1910 – 1930), decreasing thereafter until 1965, and steadily increasing again, perhaps somewhat due to or at least connected with the changing nature of the SOI relationship (Fig. 11). This is contrast to summer (Fig. 12), which shows persistent weak trends, with unique decreases in pressure across the entire continent over the last 50 years.

4. Discussion and Conclusions

Examining the reconstructed pressure over the 20th century details new information on the range and scope of natural and potentially forced variability in Antarctic pressure on longer timescales than before. When compared to gridded pressure datasets that span the 20th century, the pressure reconstructions agree the best with HadSLP2, with generally the highest correlations, smallest biases, and lowest RMSEs. There are also less differences in the HadSLP2 statistics between pre- and post-1950 and the anomalies in certain important years align the best with the reconstructions; in contrast, ERA-20C seems to have the largest differences with our reconstructions. Part of this difference may be superficial however in the sense that both HadSLP2 and our reconstructions are based on similar statistical techniques.

Throughout the 20th century, summer pressures tend to be uniform across the continent, with a high degree of spatial correlation. The earlier part of the 20th century was marked by several years of anomalous high pressure across the continent. In particular, the summer 1925/1926 showed large pressure anomalies generally > 6 hPa in the reconstructions across all of the continent, aligning with a strong positive SAM index from two SAM reconstructions [*Jones et al.*, 2009], as well as a moderate El Niño year. During the second half of the 20th century, the most notable feature in Antarctic summer pressures is a steady decrease, beginning around 1960, and likely tied to stratospheric ozone depletion [*Thompson and Solomon*, 2002]. The reconstructions add to this story by demonstrating that the observed trends, particularly during 1970-1999, were the lowest trends at the majority of locations since 1905, falling below the 95% confidence of the best estimate for historic trends in the reconstructions.

While there are not unique and persistent trends in winter, the main story from this season over the entire 20th century is the role of natural variability. Correlations with the SAM along the Antarctic Peninsula, and the SOI throughout all of Antarctica, change more dramatically in this season than they do in summer. During the first half of the 20th century, interannual pressure variability was reduced compared to the second half, particularly over the Antarctic interior. Additionally, pressure variability across the Antarctic Peninsula is much more independent / unrelated to pressure variability across the remainder of Antarctica, different to the more uniform structure seen in summer. Natural variability appears to play a dominant measure of historical winter Antarctic pressure variability, with noted multi-decadal variations in mean pressure (clearly seen in low-frequency smoothed versions of the reconstructions) as well as in running trends time series.

As suggested in the discussion, ongoing and future work includes investigating various climate model simulations with isolated forcing mechanisms to understand the role each play in historical Antarctic pressure variations throughout the 20th century. Notably, these simulations will investigate the role of tropical sea surface temperature variability, and therefore help to shed light on the role of interannual and even multi-decadal fluctuations in tropical SSTs, which have been shown recently to be an important player in ongoing Antarctic climate variability [*Ding et al.*, 2011; *Ding and Steig*, 2013; *Li et al.*, 2014; *Clem and Fogt*, 2015]. Additional work is planned for the construction of a continent-wide, seasonal gridded reconstruction, to provide more local details on historical pressure across the continent. This spatial reconstruction will be guided in part by the reconstructions presented here and in our companion paper [*Fogt et al.*, 2016], and hopefully will provide further information on understanding the ongoing changes across the Antarctic continent in a longer, more observationally-constrained context than before.

Acknowledgments

All authors but JMJ acknowledge support from NSF grant #1341621. Thanks are extended to ECMWF for their reanalysis data (http://apps.ecmwf.int/datasets/), the British Antarctic Survey for hosting the Antarctic READER data (https://legacy.bas.ac.uk/met/READER/), NOAA Earth System Research Laboratory for the 20th Century Reanalysis data

(http://www.esrl.noaa.gov/psd/data/gridded/data.20thC_ReanV2c.html), the UK Hadley Centre for HadSLP2 data (http://www.metoffice.gov.uk/hadobs/hadslp2/), and the NCAR/UCAR research data archive for the majority of mid-latitude pressure data (http://rda.ucar.edu/datasets/ds570.0/#!description). The pressure reconstructions generated and evaluated here can be made available by request through email to the corresponding author RLF (fogtr@ohio.edu).

References

Abram, N. J., E. R. Thomas, J. R. McConnell, R. Mulvaney, T. J. Bracegirdle, L. C. Sime, and A. J. Aristaraom (2010), Ice core evidence for a 20th century decline of sea ice in the Bellingshausen Sea, Antarctica, *J. Geophys. Res.*, *115*, doi:10.1029/2010JD014644.

Abram, N. J., R. Mulvaney, F. Vimeux, S. J. Phipps, J. Turner, and M. H. England (2014), Evolution of the Southern Annular Mode during the past millennium, *Nat. Clim. Change*, *4*, 564-569, doi:10.1038/nclimate2235.

Allan, R. J., and T. J. Ansell (2006), A new globally complete monthly historical mean sea level pressure data set (HadSLP2): 1850-2004, *J. Clim.*, *19*, 5816-6842.

Arblaster, J. M., and G. A. Meehl (2006), Contributions of External Forcings to Southern Annular Mode Trends, *J. Clim.*, *19*, 2896–2905, doi:10.1175/JCLI3774.1.

Bracegirdle, T. J., J. Turner, J. S. Hosking, T. Phillips (2014), Sources of uncertainty in projections of 21st century westerly wind changes over the Amundsen Sea, West Antarctica, in CMIP5 climate models, *Clim. Dyn.*, *43*, 2093-2104, doi:10.1007/s00382-013-2023-1.

Bracegirdle, T. J., N. Bertler, A. M. Carleton, Q. Ding, C. J. Fogwill, J. C. Fyfe, H. H. Hellmer, A. Y. Karpechko, K. Kusahara, E. Larour, P. A. Mayewski, W. N. Meier, L. M. Polvani, J. L. Russell, S. L. Stevenson, J. Turner, J. M. van Wessem, W. J. van de Berg, and I. Wainer (2016), A multi-disciplinary perspective on climate model evaluation for Antarctica, *Bull. Amer. Meteorol. Soc.*, doi:10.1175/BAMS-D-15-00108.1, in press.

Clem, K. R., and R. L. Fogt (2013), Varying roles of ENSO and SAM on the Antarctic Peninsula climate in austral spring, *J. Geophys. Res.*, *118*, 11, 481–11,492, doi:10.1002/jgrd.50860.

Clem, K. R., and R. L. Fogt (2015), South Pacific circulation changes and the connection to the tropics and regional Antarctic warming in austral spring, 1979-2012, *J. Geophys. Res.*, *120*, 2773-2792, doi:10.1002/2014JD022940.

Compo, G. P. et al. (2011), The Twentieth Century Reanalysis Project, *Q. J. R. Meteorol. Soc.*, *137*, 1-28, doi:10.1002/qj.776.

Ding, Q. and E. J. Steig (2013), Temperature change on the Antarctic Peninsula linked to the Tropical Pacific, *J. Clim.*, *26*, 7570–7585, doi:10.1175/JCLI-D-12-00729.1.

Ding, Q., E. J. Steig, B. S. Battisti, and M. Küttel (2011), Winter warming in West Antarctica caused by central tropical Pacific warming, *Nat. Geosci.*, *4*, 398-403. doi:10.1038/ngeo1129.

Fogt, R. L., and D. H. Bromwich (2006), Decadal variability of the ENSO teleconnection to the high latitude South Pacific governed by coupling with the Southern Annular Mode, *J. Clim.*, *19*, 979-997.

Fogt, R.L., and E. A. Zbacnik (2014), Sensitivity of the Amundsen Sea Low to stratospheric ozone depletion, *J. Clim.*, *27*, 9383–9400. doi:10.1175/JCLI-D-13-00657.1.

Fogt, R. L., and A. J. Wovrosh (2015), The relative influence of tropical sea surface temperatures and radiative forcing on the Amundsen Sea Low, *J. Clim.*, *28*, 8540-8555, doi:10.1175/JCLI-D-15-0091.1.

Fogt, R. L., J. Perlwitz, A. J. Monaghan, D. H. Bromwich, J. M. Jones, and G. J. Marshall (2009), Historical SAM variability, part II: 20th century variability and trends from reconstructions, observations, and the IPCC AR4 models, *J. Clim.*, *22*, 5346-5365.

Fogt, R. L., D. H. Bromwich, and K. M. Hines (2011), Understanding the SAM influence on the South Pacific ENSO teleconnection, *Clim Dyn.*, *36*, 1555-1576.

Fogt, R. L., J. M. Jones, and J. Renwick (2012), Seasonal zonal asymmetries in the Southern Annular Mode and their impact on regional temperature anomalies, *J. Clim.*, *25*, 6253-6270.

Fogt, R. L., C. A. Goergens, M. E. Jones, G. Witte, M. Y. Lee, and J. M. Jones (2016), Antarctic Station Based Seasonal Pressure Reconstructions Since 1905, Part 1: Reconstruction evaluation, *J. Geophys. Res.,* in review.

Hosking, J. S., A. Orr, G. J. Marshall, J. Turner, and T. Phillips (2013), The influence of the Amundsen-Bellingshausen Seas Low on the climate of West Antarctica and its representation in coupled climate model simulations, *J. Clim.*, *26,* 6633-6648.

Jones, J. M., and M. Widmann (2003), Instrumental- and tree-ring based estimates for the Antarctic Oscillation, *J. Clim.*, *16*, 3511-3524.

Jones, J. M., and M. W. Widmann (2004), Atmospheric Science- Early peak in Antarctic oscillation index, *Nature*, *432*, 290-291.

Jones, J. M., R. L. Fogt, M. Widmann, G. Marshall, P. D. Jones, and M., Visbeck (2009), Historical SAM Variability. Part I: Century Length Seasonal Reconstructions, *J. Clim.*, *22*, 5319-5345.

Karoly, D.J. (1989), Southern Hemisphere circulation features associated with El Niño-Southern Oscillation events, *J. Clim.*, *2*, 1239–1252.

Li, X., D. M. Holland, E. P. Gerber, and C. Yoo (2014), Impacts of the north and tropical Atlantic Ocean on the Antarctic Peninsula and sea ice, *Nature*, *505*, 538-542.

Marshall, G. J. (2003), Trends in the Southern Annular Mode from observations and reanalyses, *J. Clim.*, *16*, 4134–4143.

Marshall, G. J., and T. J. Bracegirdle (2015), An examination of the relationship between the Southern Annular Mode and Antarctic surface air temperatures in the CMIP5 historical runs, *Clim. Dyn.*, *45*, 1513-1535. 10.1007/s00382-014-2406-z.

Marshall, G. J., S. Di Battista, S. S. Naik, M. Thamban (2011), Analysis of a regional change in the sign of the SAM-temperature relationship in Antarctica, *Clim. Dyn.*, *36*, 277-287. 10.1007/s00382-009-0682-9.

Miller, R. L., G. A. Schmidt, and D. T. Shindell (2006), Forced annular variations in the 20th century Intergovernmental Panel on Climate Change Fourth Assessment Report models, *J. Geophys. Res.*, *111,* doi:10.1029/2005JD006323.

Murphy, E. J., A. Clarke, N. J. Abram, and J. Turner (2014), Variability of sea-ice in the northern Weddell Sea during the 20th century, *J. Geophys. Res.*, *119*, 4549–4572, doi:10.1002/2013JC009511.

Perlwitz, J., S. Pawson, R. L. Fogt, J. E. Nielsen, and W. D. Neff (2008), Impact of stratospheric ozone hole recovery on Antarctic climate. *Geophys. Res. Lett.*, *35*, L08714, doi: 10.1029/2008GL033317.

Schneider, D. P., and E. J. Steig (2008), Ice cores record significant 1940s warmth related to tropical climate variability, *Proc. Nat. Acad. Sci., 105*, 12154-12158, doi:10.1073/pnas.0803627105.

Solomon, S. and C. R. Stearns (1999), On the role of the weather in the deaths of R. F. Scott and his companions. *Proc. Natl. Acad. Sci., 96*, 13012-13016.

Stammerjohn, S. E., D. G. Martinson, R. C. Smith, X. Yuan, and D. Rind (2008), Trends in Antarctic annual sea ice retreat and advance and their relation to El Niño Southern Oscillation and Southern Annular Mode variability, *J. Geophys. Res.*, *113*, doi:10.1029/2007JC004269.

Thomas, E. R., G. J. Marshall, and J. R. McConnell (2008), A doubling in snow accumulation in the western Antarctic Peninsula since 1850, *Geophys. Res. Lett.*, *35*, L01706, doi:10.1029/2007GL032529.

Thompson, D. W. J., and S. Solomon (2002), Interpretation of recent Southern Hemisphere climate change, *Science*, *296*, 895-899.

Trenberth, K. E., and J. M. Caron (2000), The Southern Oscillation revisited: Sea level pressures, surface temperatures, and precipitation, *J. Clim.*, *13*, 4358-4365.

Turner, J. (2004), The El Nino-Southern Oscillation and Antarctica, *Int. J. Climatol*., *24*, 1-31.

Turner, J., J.C. Comiso, G.J. Marshall, T.A. Lachlan-Cope, T. Bracegirdle, T. Maksym, M.P. Meredith, Z. Wang, and A. Orr (2009), Non-annular atmospheric circulation change induced by stratospheric ozone depletion and its role in the recent increase of Antarctic sea ice extent, *Geophys. Res. Lett.*, *36*, L08502, doi:10.1029/2009GL037524.

Turner, J., T. J. Bracegirdle, T. Phillips, G. J. Marshall, J. S. Hosking (2013), An initial assessment of Antarctic sea ice extent in the CMIP5 models, *J.Clim.*, *26*, 1473-1484, doi:10.1175/JCLI-D-12-00068.1.

Turner, J., J. S. Hosking, G. J. Marshall, T. Phillips, and T. J. Bracegirdle (2015a), Antarctic sea ice increase consistent with intrinsic variability of the Amundsen Sea Low, *Clim. Dyn.*, doi:10.1007/s00382-015-2708-9.

Turner, J., J. S. Hosking, T. J. Bracegirdle, G. J. Marshall, and T. Phillips (2015b), Recent changes in Antarctic sea ice, *Phil. Trans. Roy. Soc. London, A*, *373*, doi:10.1098/rsta.2014.0163.

Villalba, R., A, Lara, M. H. Masiokas, R. Urrutia, B. H. Luckman, G. J. Marshall, I. A. Mundo, D. A Christie, E. R. Cook, R. Neukom, K. Allen, P. Fenwick, J. A. Bininsegna, Am. M. Srur, M. S. Morales, D. Araneo, J. G. Palmer, E. Cuq, J. C. Aravena, A. Holz, and C. Lequesne (2012), Unusual Southern Hemisphere tree growth patterns induced by changes in the Southern Annular Mode, *Nat. Geosci.*, *5*, 793-798.

Visbeck, M. (2009), A station-based Southern Annular Mode index from 1884 to 2005, *J. Clim.*, *22*, 940-950.

Wilson, A. B., D. H. Bromwich, K. M. Hines, and S. Wang (2014), El Niño flavors and their simulated impacts on atmospheric circulation in the high southern latitudes, *J. Clim.*, *27*, 8934-8955.

Zazulie, N., M. Rusticucci, S. Solomon (2010), Changes in climate at high southern latitudes: A unique daily record at Orcadas spanning 1903-2008, *J. Clim.*, *23*, 189-196, doi:10.1175/2009JCLI3074.1.

Figure captions.

Figure 1. Location of the 17 Antarctic stations where the seasonal reconstructions are investigated in this paper. The coloring indicates geographic groupings where several stations are averaged together to investigate the historical pressure variability over a region. See text for details.

Figure 2. The correlation, bias, and RMSE (columns) by season (rows) between the reconstructions and the bilinearly interpolated gridded pressure data from 20CR (black lines), ERA-20C (red lines), and HadSLP2 (blue lines). The x-axis gives the station, working east around Antarctica from the Peninsula (Fig. 1). 'Early' represents statistics calculated during 1905-1956, while 'late' represents statistics calculated during 1957-end of the data / reconstruction (varies between 2010-2013). Surface pressure was employed for the bias / RMSE calculations at Vostok and Amundsen-Scott (stations 16 and 17, respectively), and therefore no calculations were performed for these statistics and locations using HadSLP2.

Figure 3. Time series of region-averaged sea level pressure for DJF, with the best original reconstructions plotted in red and the best pseudo-reconstruction plotted in blue. The regions are defined as in Fig. 1, with DML = Dronning Maud Land. Shading represents the maximum extent of the 95% confidence intervals around both the original and pseudo reconstructions, and the correlations in each panel are the correlations between the region-averaged reconstructions and observations. The year on the x-axis represents the year of the December (i.e., 1920 = December 1920 – February 1921).

Figure 4. Sea level pressure anomalies during DJF 1925/26 based on a) 20CR b) ERA-20C and c) HadSLP2. Shading in each panel represents the number of standard deviations the anomalies are from the 1981-2010 mean. Also plotted are the anomalies for sea level pressure observations in the midlatitudes, and for the original reconstructions over Antarctica (with the size and color representing the magnitude of the anomaly as given by the label bar). Note that Orcadas, northeast of the Antarctic Peninsula, is an observed anomaly, not a reconstruction. Also, for the interior stations (Byrd, Vostok, and Amundsen-Scott), surface pressure anomalies are plotted.

Figure 5. As in Fig. 3, but after smoothing the interannual sea level pressure values with an 11-yr Hamming filter.

Figure 6. As in Fig. 3, but for JJA.

Figure 7. As in Fig. 4, but for JJA 1938, with the pseudo-reconstruction anomalies plotted over Antarctica.

Figure 8. As in Fig. 5, but for JJA.

Figure 9. Reconstructed (original in red, pseudo in blue) averaged pressure anomalies for the Antarctic Interior stations of Amundsen-Scott and Vostok, along with the observations in black. a) DJF anomalies b) 11-yr smoothed DJF anomalies c) JJA anomalies d) 11-yr smoothed JJA anomalies.

Figure 10. Antarctic regional mean 30-year running correlations of the pressure reconstructions with the Fogt (solid lines) and JW Concat (dashed lines) SAM index reconstructions [from *Jones et al.*, 2009] for DJF (red lines) and JJA (blue lines). Dashed horizontal black lines indicate 30-yr correlations significantly different than zero at $p<0.05$.

Figure 11. As in Fig. 10, but for Antarctic regional mean 30-year running correlations between the pressure reconstructions and the SOI.

Figure 12. DJF Antarctic regional mean 30-year running trends for observations (black lines) and original and pseudo reconstructions (red and blue, respectively). The x-axis identifies the starting year of the 30-year trend. The gray shading represents the 95% confidence interval for the best estimate of the 30-year pressure trends based on the goodness of fit between the observed and reconstructed pressures during the period of overlap.

Figure 13. As in Fig. 12, but for JJA.

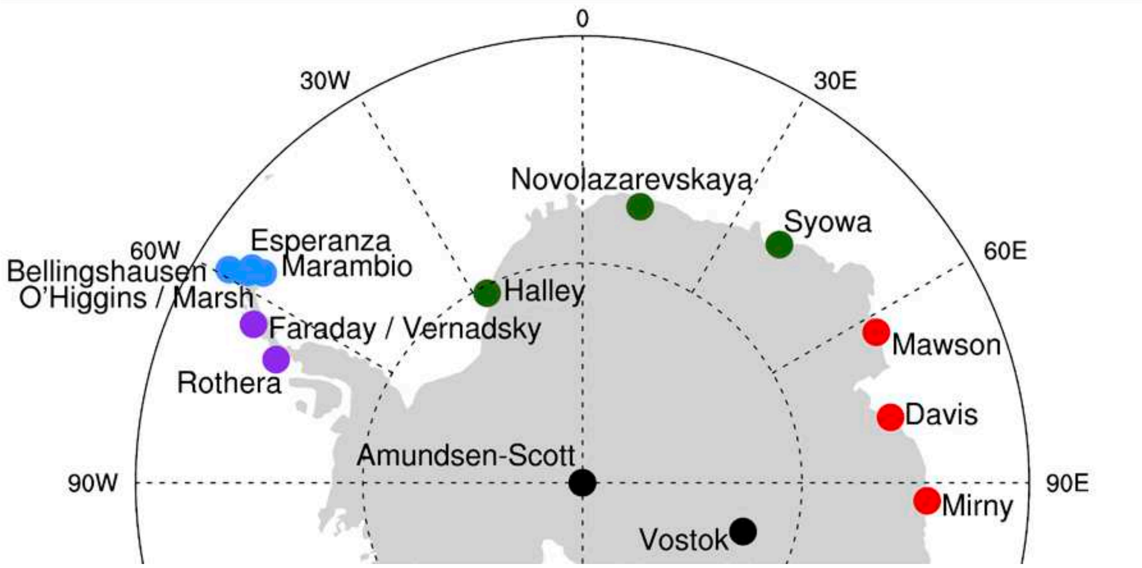

Figure 1. Location of the 17 Antarctic stations where the seasonal reconstructions are investigated in this paper. The coloring indicates geographic groupings where several stations are averaged together to investigate the historical pressure variability over a region. See text for details.

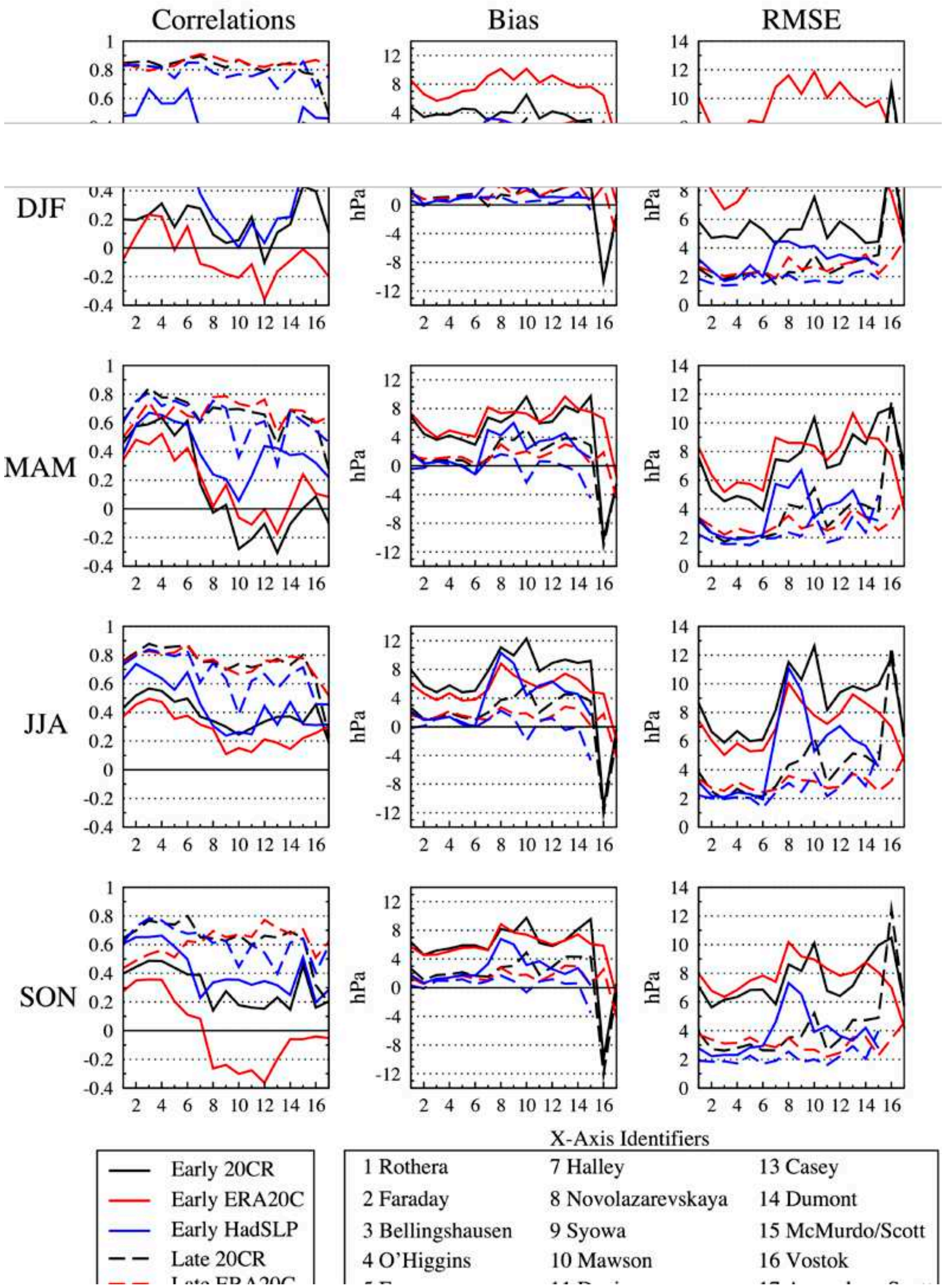

Figure 2. The correlation, bias, and RMSE (columns) by season (rows) between the reconstructions and the bilinearly interpolated gridded pressure data from 20CR (black lines), ERA-20C (red lines), and HadSLP2 (blue lines). The x-axis gives the station, working east around Antarctica from the Peninsula (Fig. 1). 'Early' represents statistics calculated during 1905-1956, while 'late' represents statistics calculated during 1957-end of the data / reconstruction (varies between 2010-2013). Surface pressure was employed for the bias / RMSE calculations at Vostok and Amundsen-Scott (stations 16 and 17, respectively), and therefore no calculations were performed for these statistics and locations using HadSLP2.

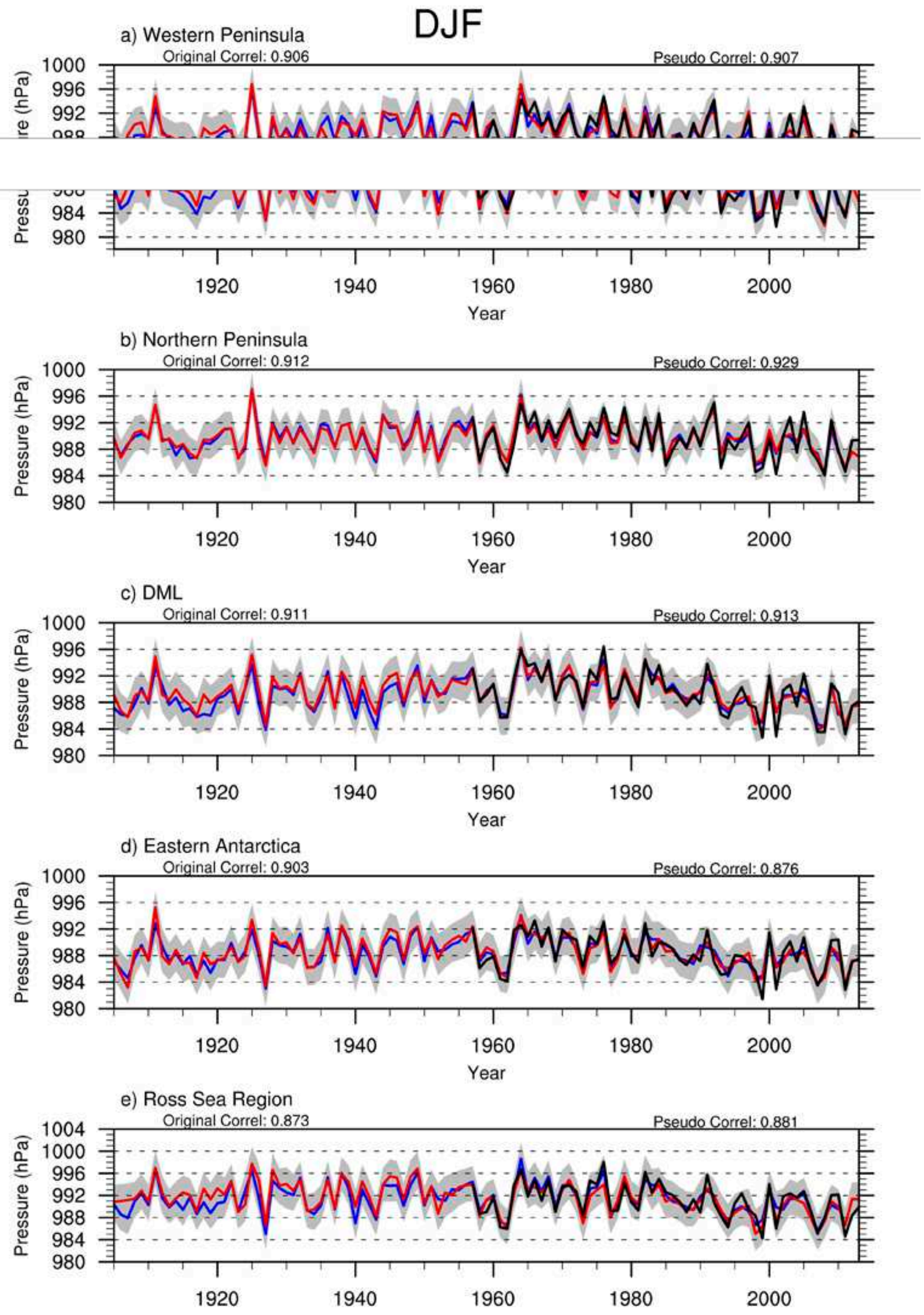

Figure 3. Time series of region-averaged sea level pressure for DJF, with the best original reconstructions plotted in red and the best pseudo-reconstruction plotted in blue. The regions are defined as in Fig. 1, with DML = Dronning Maud Land. Shading represents the maximum extent of the 95% confidence intervals around both the original and pseudo reconstructions, and the correlations in each panel are the correlations between the region-averaged reconstructions and observations. The year on the x-axis represents the year of the December (i.e., 1920 = December 1920 – February 1921).

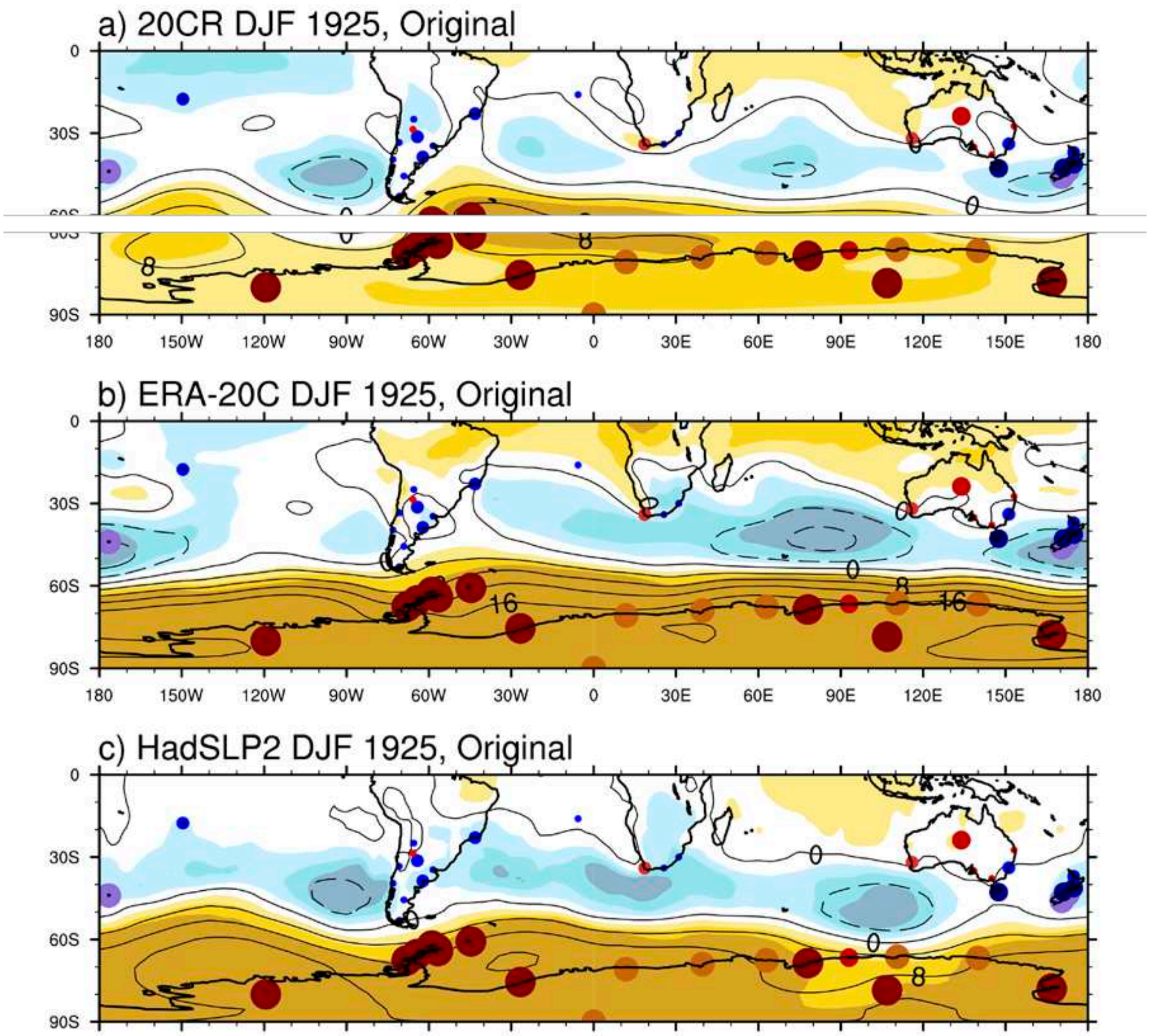

Figure 4. Sea level pressure anomalies during DJF 1925/26 based on a) 20CR b) ERA-20C and c) HadSLP2. Shading in each panel represents the number of standard deviations the anomalies are from the 1981-2010 mean. Also plotted are the anomalies for sea level pressure observations in the midlatitudes, and for the original reconstructions over Antarctica (with the size and color representing the magnitude of the anomaly as given by the label bar). Note that Orcadas, northeast of the Antarctic Peninsula, is an observed anomaly, not a reconstruction. Also, for the interior stations (Byrd, Vostok, and Amundsen-Scott), surface pressure anomalies are plotted.

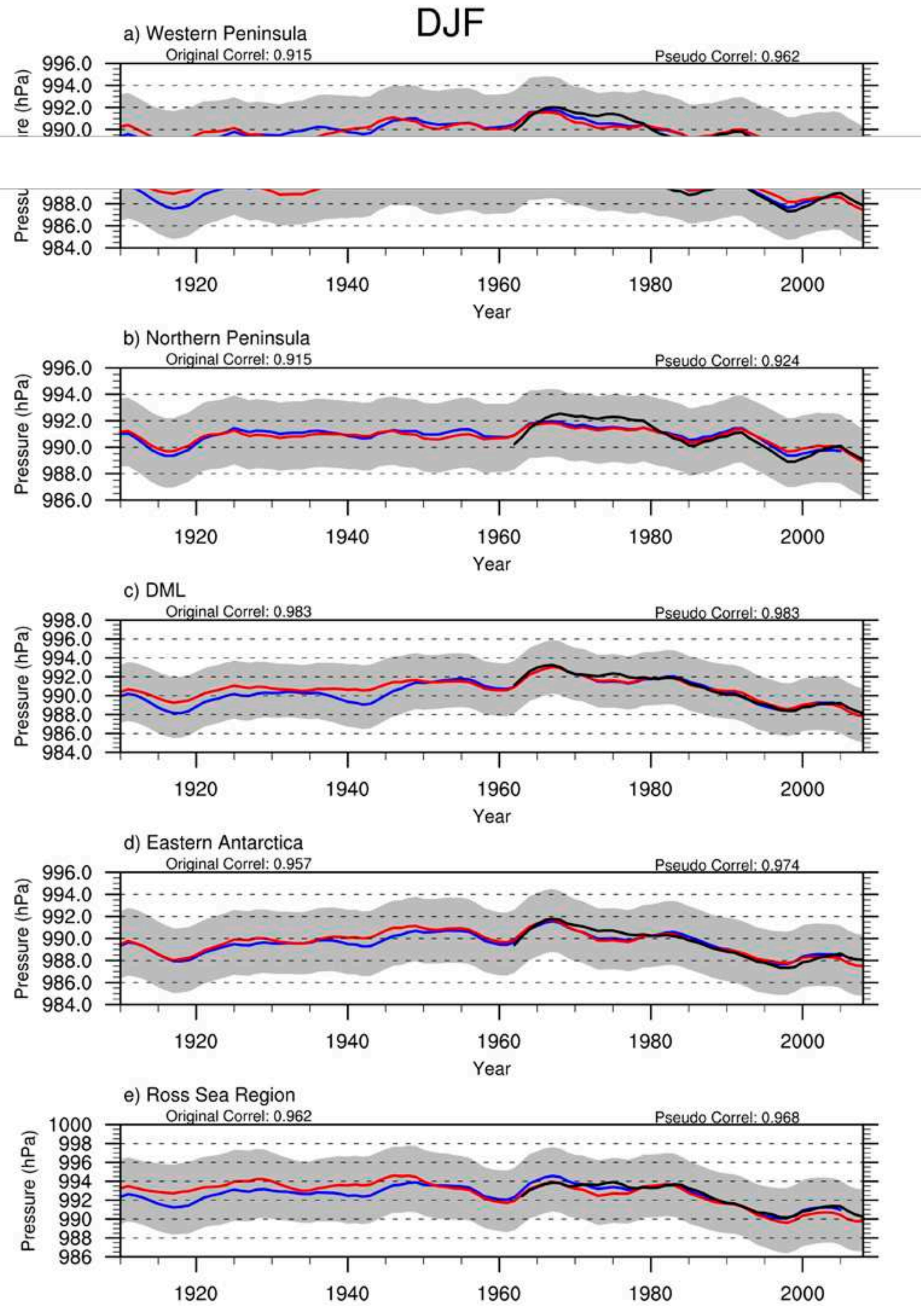

Figure 5. As in Fig. 3, but after smoothing the interannual sea level pressure values with an 11-yr Hamming filter.

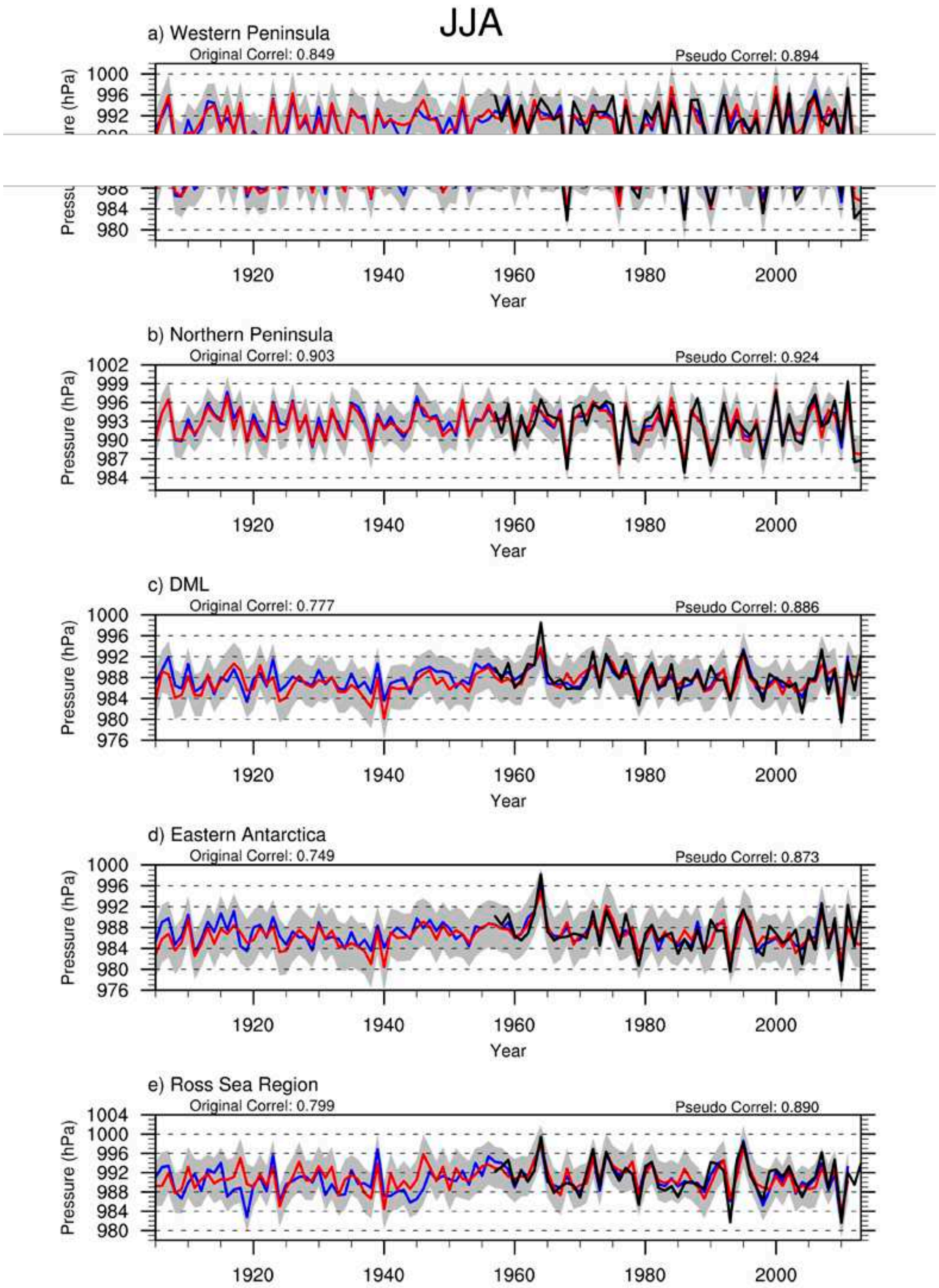

800
801 **Figure 6.** As in Fig. 3, but for JJA.
802

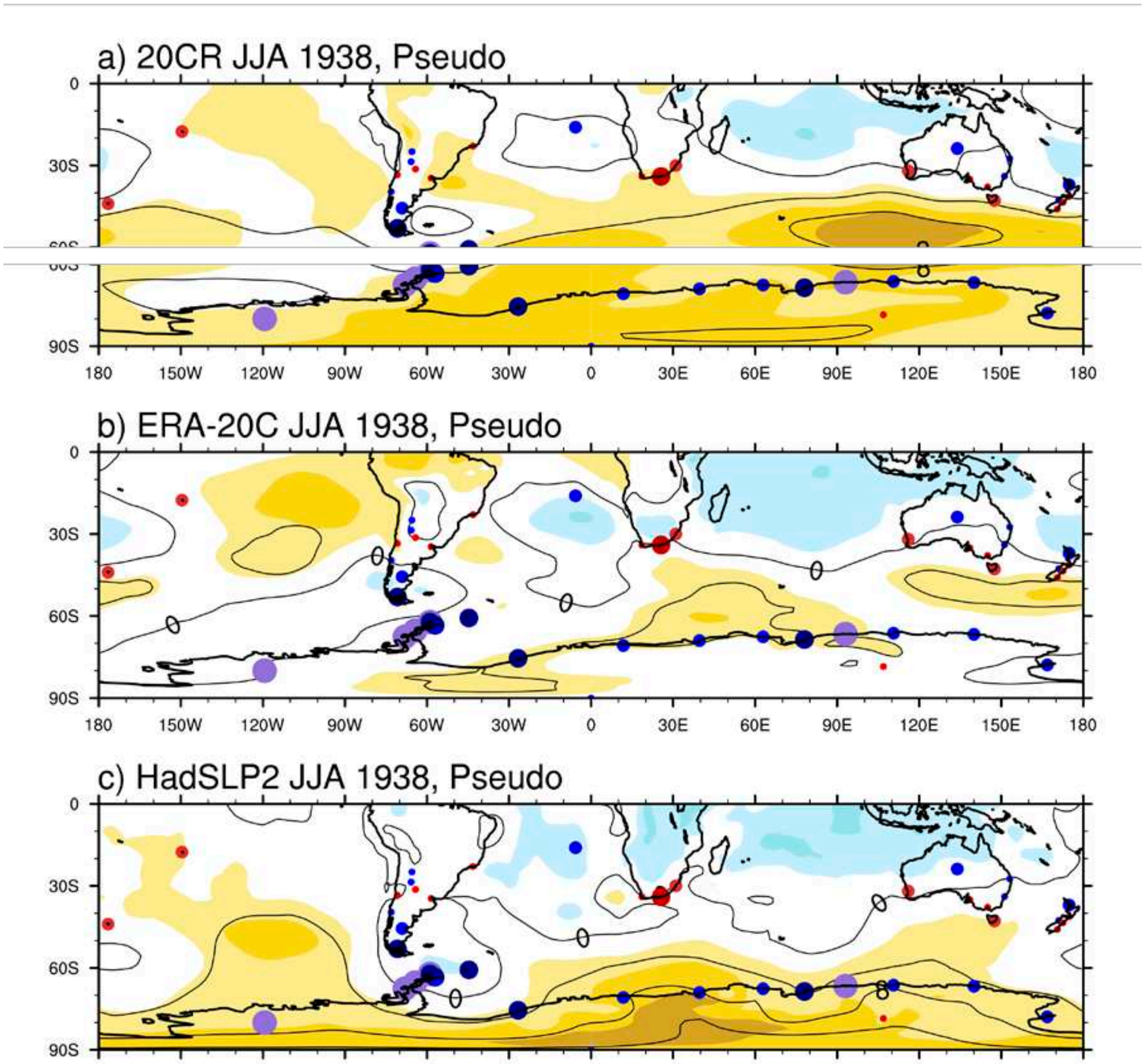

Figure 7. As in Fig. 4, but for JJA 1938, with the pseudo-reconstruction anomalies plotted over Antarctica.

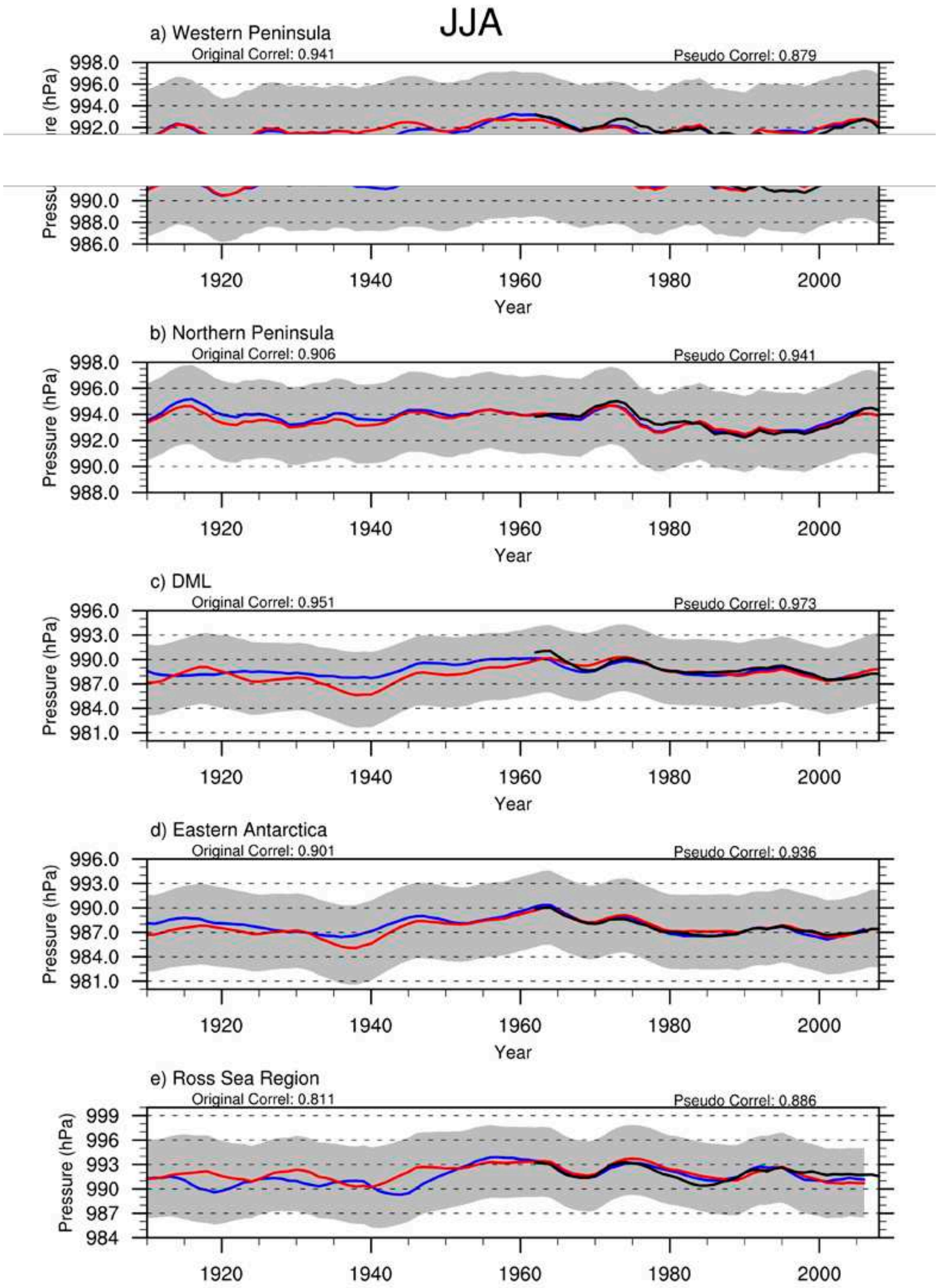

807 **Figure 8.** As in Fig. 5, but for JJA.
808

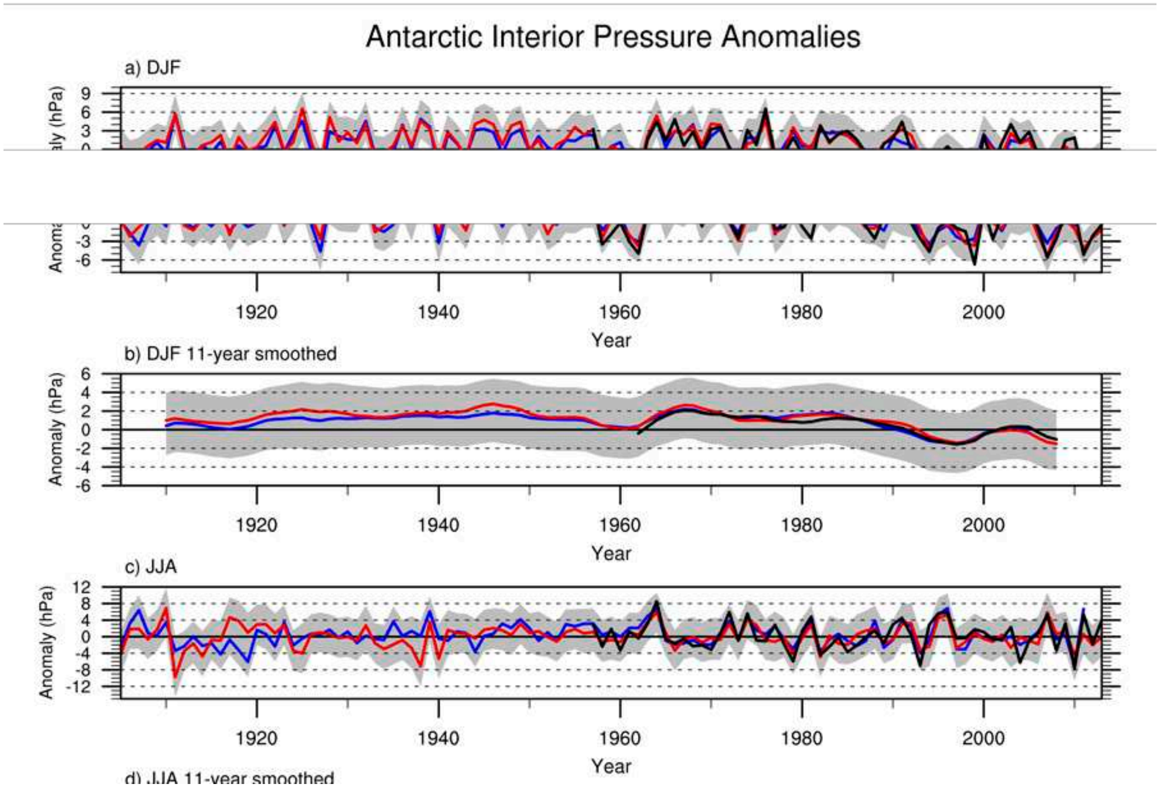

Figure 9. Reconstructed (original in red, pseudo in blue) averaged pressure anomalies for the Antarctic Interior stations of Amundsen-Scott and Vostok, along with the observations in black. a) DJF anomalies b) 11-yr smoothed DJF anomalies c) JJA anomalies d) 11-yr smoothed JJA anomalies.

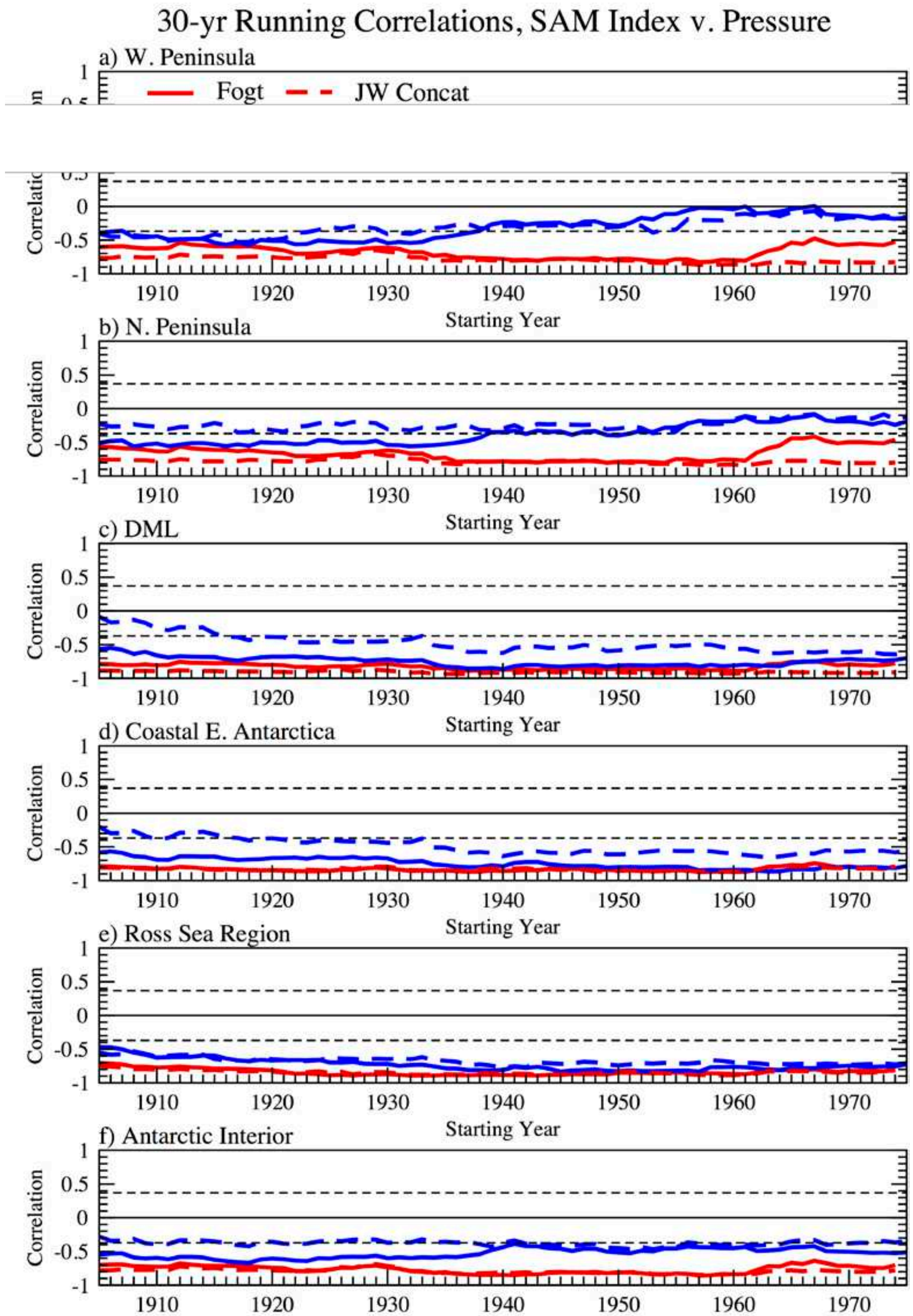

Figure 10. Antarctic regional mean 30-year running correlations of the pressure reconstructions with the Fogt (solid lines) and JW Concat (dashed lines) SAM index reconstructions [from *Jones et al.*, 2009] for DJF (red lines) and JJA (blue lines). Dashed horizontal black lines indicate 30-yr correlations significantly different than zero at $p<0.05$.

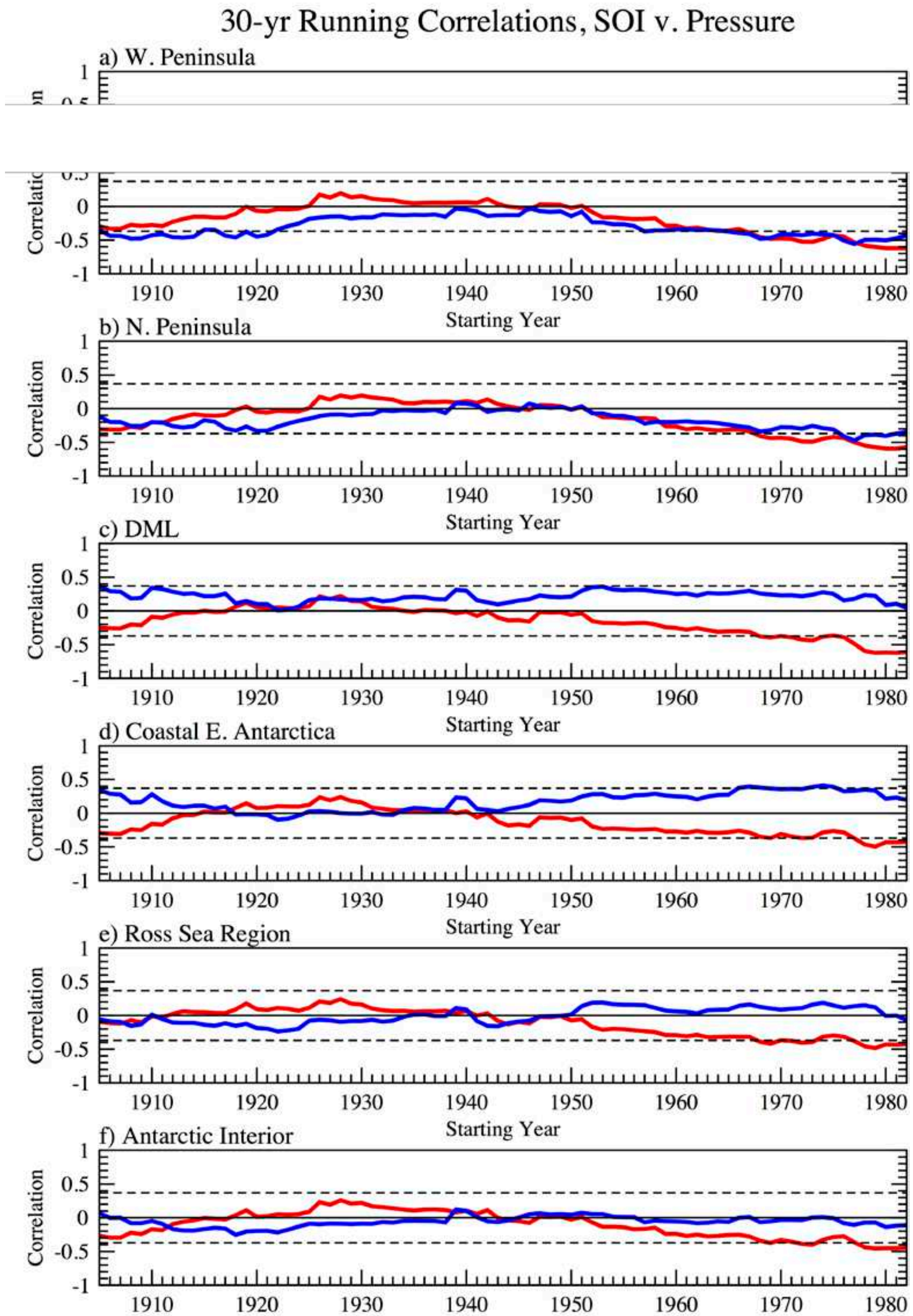

Figure 11. As in Fig. 10, but for Antarctic regional mean 30-year running correlations between the pressure reconstructions and the SOI.

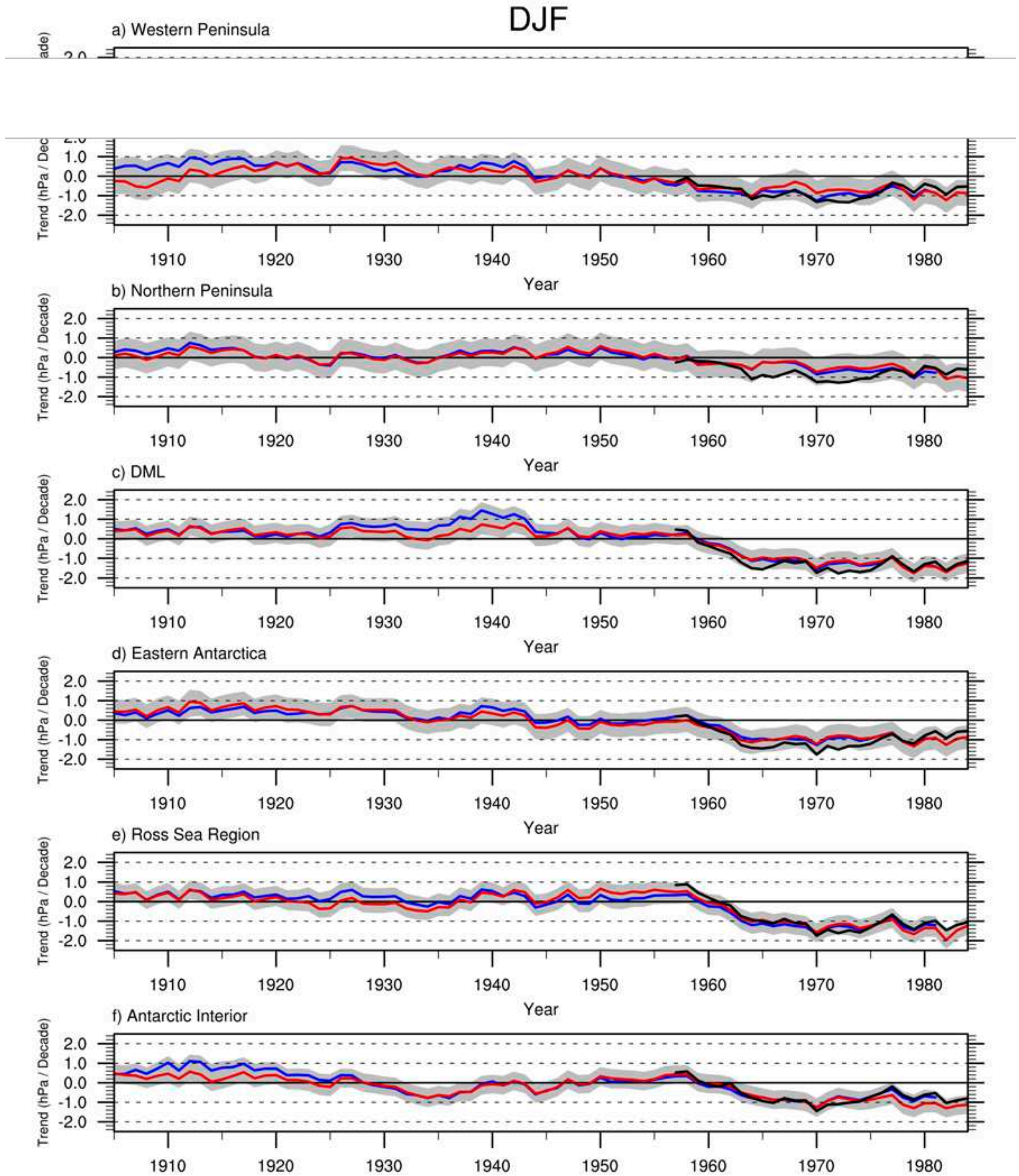

Figure 12. DJF Antarctic regional mean 30-year running trends for observations (black lines) and original and pseudo reconstructions (red and blue, respectively). The x-axis identifies the starting year of the 30-year trend. The gray shading represents the 95% confidence interval for the best estimate of the 30-year pressure trends based on the goodness of fit between the observed and reconstructed pressures during the period of overlap.

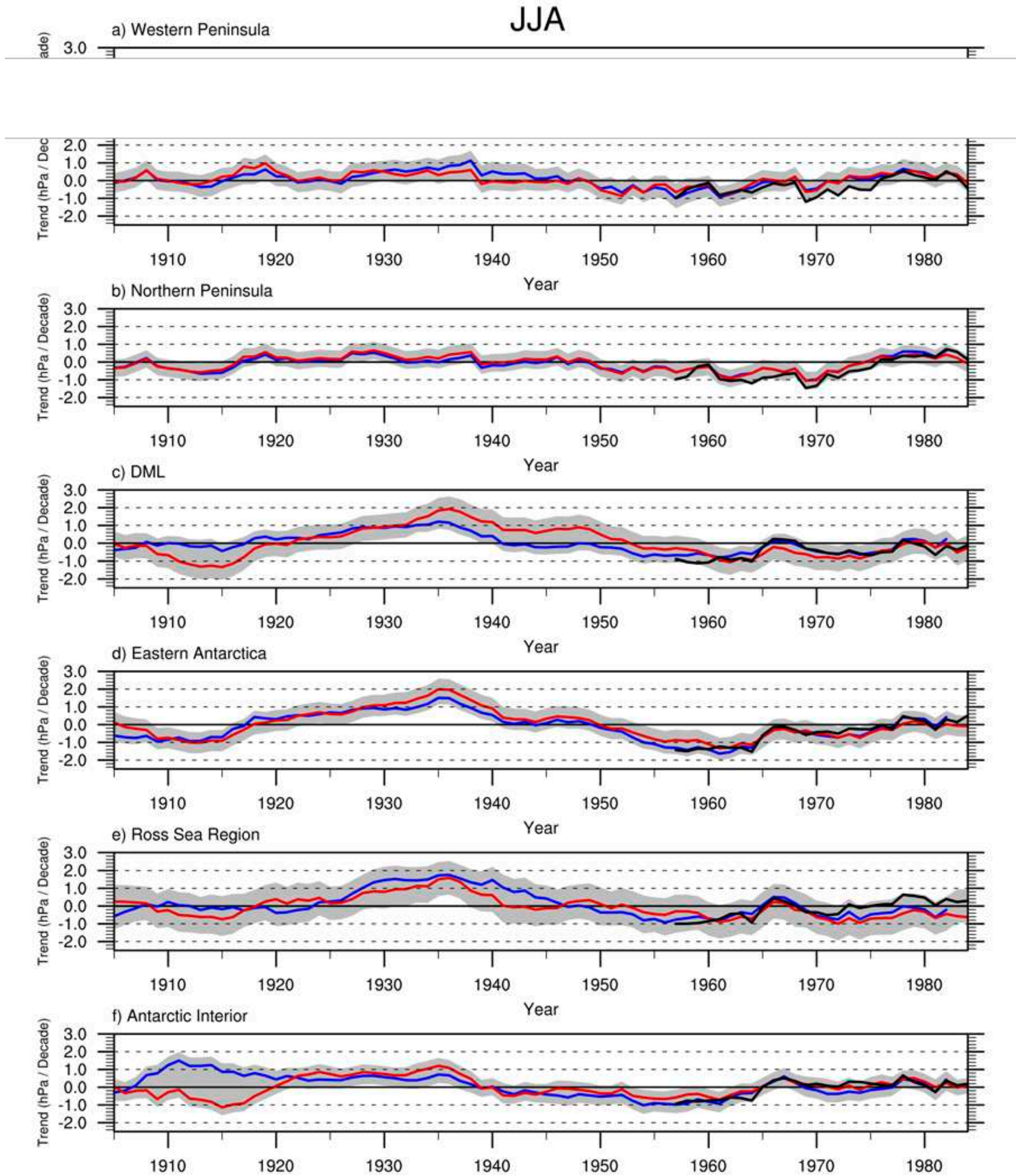

831
832 **Figure 13.** As in Fig. 12, but for JJA.